Local Structure around Cr^{3+} Ions in Dilute Acetate and Perchlorate Aqueous Solutions

Maxim I. Boyanov*,†,‡ Kenneth M. Kemner†, Tomohiro Shibata‡, and Bruce A. Bunker‡

Environmental Research, Argonne National Laboratory, Argonne, Illinois 60439, and Department of Physics, University of Notre Dame, Notre Dame, Indiana 46556

Received: February 6, 2004; In Final Form: April 7, 2004

The hydration structure and aqueous acetate complexation of Cr^{3+} ions were studied by X-ray absorption fine structure (XAFS) spectroscopy as a function of pH, concentration, acetate:Cr ratio, and age of the solution. In the perchlorate solutions, we found an octahedral hydration shell around the Cr^{3+} ion at 1.96 Å, confirming previous results through an independent analysis. Distinct Cr−Cr correlation was observed in the Cr acetate solutions, indicating that acetate groups bridge between the metal ions in a polymer structure. Modeling of the data confirmed a cyclic trichromium complex in acetate solutions. Similar spectral features in the Fourier transform were observed at 3.0−3.5 Å for both hydrated and polynuclear Cr. Comparison of the spectral content of such features in the two different cases showed that the origin of the 3.0−3.5 Å structure is multiple scattering within the first O shell alone. Thus, no spectral contribution could be attributed to the outer hydration molecules in data for hydrated Cr^{3+}. We also report on differences in first-shell O backscattering (or possible spectral contributions from H atoms) in the aqueous solutions relative to the crystal oxide, determined by systematic analysis of a Cr_2O_3 standard.

Introduction

In many areas of science, it is necessary to model the properties of aqueous solutions. Continuum models were found insufficient in that respect,[1] pointing to the importance of the hydration structure studies carried out for many elements during the last three decades.[2,3] Understanding aqueous metal adsorption to mineral and biological surfaces also requires structural information, as the process is determined by the solvated ion's form, size, and availability in solution, as well as by the geometry of the complex it forms with surface functional groups.

The structure of hydrated Cr^{3+} has been investigated previously by X-ray and neutron techniques.[4−16] An octahedral hydration sphere was determined, with a Cr−O distance of 1.97−1.98 Å.[4−7] Because of the unusually long residence time of Cr inner hydration molecules ($\sim 10^6$ s),[17] an outer hydration sphere distinct from bulk water can be formed. Evidence for this has been provided by scattering,[4,8−10] vibration spectroscopy,[11] NMR,[12] and transport studies.[13] More recently, the structure of dilute Cr solutions (as low as 0.005 M) has been investigated by X-ray absorption fine structure (XAFS) spectroscopy and contributions from second-hydration-shell molecules were reported in the spectra.[5,14−16]

Metal−acetate complexation in solution has been studied previously by Fourier transform infrared (FT-IR) spectroscopy.[18] The technique correlates shifts in the carboxylate stretching frequencies with the binding mode in known crystalline compounds[19,20] and applies this dependence to solution complexes. On this basis, the aqueous metal−acetate chelation types for several ions were classified in four main groups: ionic, monodentate, bidentate, and bridging-bidentate (Figure 1). Aqueous Cr^{3+} acetate, detailed in a separate study,[21] showed dependence of the spectra on pH, acetate:metal ratio, and age of the solution. The speciation diagram derived suggests that below pH 5.4 the dominant species is a cyclic Cr trimer, $Cr_3O(Ac)_6$, in which acetate groups are in a bridging configuration between Cr^{3+} ions (Figure 1e).

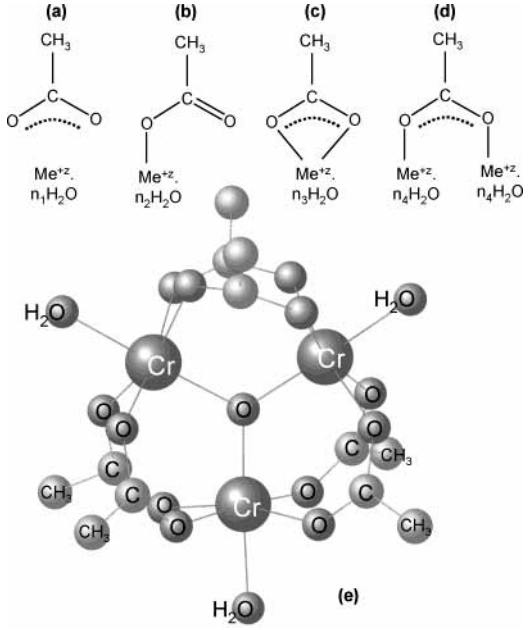

Figure 1. (a−d) Binding modes of an acetate group to a hydrated metal ion. (a) ionic, (b) monodentate, (c) bidentate, (d) bridging; dotted lines indicate the distributed electron density of the acetate group. (e) Structure of the trichromium acetate complex (bridging mode). Based on data from Chang et al.[22]

As part of our efforts to understand metal adsorption to carboxyl-rich bacterial surfaces, we began an XAFS study of metal−acetate complexes in aqueous solution.[23] In the present work, we investigate the hydration and acetate complexation of Cr^{3+} in 0.03−0.3 M aqueous solutions. The aim is to confirm

* To whom correspondence should be addressed. Current address: Argonne National Laboratory, Argonne, IL 60439; e-mail: mboyanov@nd.edu.

† Argonne National Laboratory.

‡ University of Notre Dame.

10.1021/jp049444y CCC: $27.50
Published on Web 05/14/2004

TABLE 1: Sample Identification Names and Composition

sample	$[Cr^{3+}]$ (M/l)	$[CH_3COO^-]$ (M/l)	pH	aged (h)
CrClO4-02-22	0.2	0.0	2.2	96
CrClO4-01-25	0.1	0.0	2.5	96
CrClO4-005-22	0.05	0.0	2.2	96
CrAc1-01-41	0.1	0.1	4.1	96
CrAc3-03-62	0.3	0.9	6.2	96
CrAc3-03-42	0.3	0.9	4.2	96
CrAc3-01-68	0.1	0.3	6.8	96
CrAc3-01-42	0.1	0.3	4.2	96
CrAc3-01-420	0.1	0.3	4.2	1
CrAc10-01-35	0.1	1.0	3.5	96
CrAc10-003-35	0.03	0.3	3.5	96
CrAc100-01-28	0.1	10.0	2.8	96

structural results found in previous work for the first hydration sphere and to determine the precise origin of XAFS features seen at larger distance in the Fourier transform of hydrated Cr spectra. On the basis of knowledge obtained for hydrated Cr, changes resulting from increased acetate availability in solution are examined to determine the mechanism of acetate−Cr complexation. Previous reports suggested polymerization of Cr when sufficient acetate was present in solution. We attempted to confirm the metal−metal correlation and study the structure of the polymer complex as a function of pH, concentration, acetate:Cr ratio, and age of the solution.

Experiment

Solutions were prepared by dissolving commercial Cr perchlorate and Cr acetate salts (Sigma-Aldrich and Alfa-Aesar, used without further purification) in distilled deionized water (18 MΩ). Three $Cr(ClO_4)_3$ solutions (0.05, 0.1, and 0.2 M) were used to study hydrated Cr^{3+} ions. A series of aqueous Cr acetate solutions with different acetate:Cr ratios and concentrations was used to observe the shift in equilibrium between hydrated and acetate-complexed ions toward the complexed species. The names, concentration, acetate:Cr ratio, and pH of the samples are given in Table 1. The water was boiled for at least 20 min to remove CO_2. Acetate overloading was achieved by adding acetic acid, and the pH was adjusted when necessary with NaOH.

The Cr K-edge XAFS experiments were carried out at the Materials Research Collaborative Access Team (MRCAT) beamline[24] of the Advanced Photon Source. The beamline undulator was tapered, and the incident energy was scanned by using the Si(111) reflection of the double-crystal monochromator in quick-scanning mode (approximately 3 min per scan for the extended region and 1 min per scan for the near-edge region). Harmonic rejection was achieved by reflection from a Rh-coated mirror. The beam was defined as 0.7 mm by 0.7 mm. Linearity tests[25] indicated less than 0.3% nonlinearity at 50% beam attenuation for the experimental setup and all samples. The beam intensity varied by less than 40%, approximately monotonically, over the energy range of the collected data. The solutions were kept in drilled Plexiglas slides sealed with Kapton film windows during the measurements. Spectra were recorded in fluorescence mode. Energy calibration was continuously monitored during data collection by using a Cr_2O_3 standard placed above the beam and in front of the defining slits.[26]

Standard data analysis procedures were followed.[27] Raw data from the beamline were aligned on the energy axis by the reference data; background was subtracted by using AUTOBK.[28] Different background removal parameters were compared to identify the most consistent procedure. Model calculations were obtained with FEFF8.[29,30] (The Cr−O and Cr−Cr backscattering amplitudes were calibrated with the Cr_2O_3 standard.) Data were modeled by using the FEFFIT program.[31]

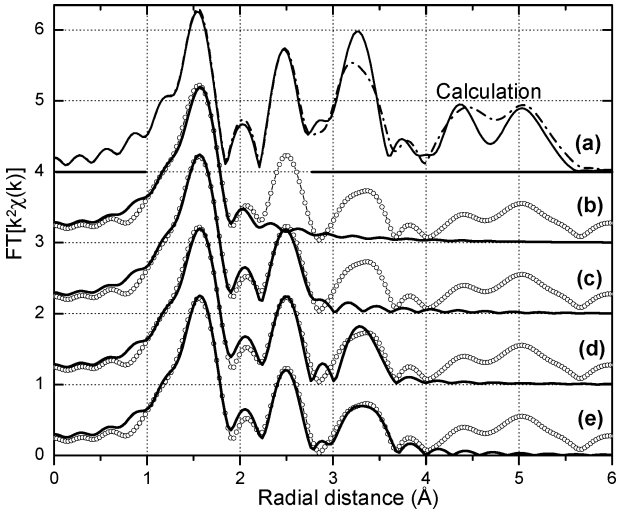

Figure 2. Comparisons of theoretical spectra (a) and modeling of Cr_2O_3 experimental data (b−e). Transform and fit parameters of the k^2-weighed data are $\Delta k = 2.8-13.5$ Å^{-1} and $\Delta R = 1.0-4.0$ Å. Shown are experimental data (symbols) and fit (lines). (a) Comparison of theoretical calculations when only SS paths are used (solid) and when MS paths are included (broken). (b) Fit with O near neighbors only. (c) Fit with O, Cr1 shells. (d) Fit with O, Cr1, Cr2 shells. (e) Fit with O, Cr1, and Cr2 shells, plus MS paths.

Results and Discussion

Cr_2O_3 Standard. Data from the Cr_2O_3 standard were used to relate features in the extended XAFS (EXAFS) spectrum of a Cr oxide compound to its known structure. The EXAFS method in X-ray spectroscopy uses the electron wave of an ejected photoelectron to probe the surroundings of the emitting atom. Electron scattering is treated in EXAFS theory by summing contributions from "scattering paths" that the electron wave can take before it returns to the central atom to interfere with itself.[27] Besides single reflections from neighbor atoms (single scattering, or SS), several scattering events can occur before the electron returns to the emitting atom (multiple scattering, or MS). The contribution of MS paths is usually negligible relative to that of SS paths, but when atoms are aligned their electron scattering ability is enhanced, and corresponding MS features appear in the spectrum. The importance of such collinear MS paths is illustrated in Figure 2a, in which Fourier transforms (FTs) of EXAFS calculations for Cr_2O_3 are compared, with and without consideration of MS paths. Differences are observed in the region 2.8−4.0 Å, where MS paths due to the octahedral O first shell contribute. Some calculated SS and MS paths might not contribute in a real sample because of loss of coherence due to thermal and structural disorder. The contribution of each path is weighed by a Debye−Waller type factor, $\exp[-2k^2\sigma^2]$, where σ is the rms deviation in path length for each path, and k is the electron wave vector.[27]

The theoretical Cr_2O_3 spectrum was calculated using the published Cr_2O_3 structure.[32] The following paths were necessary to fit the experimental spectrum: SS from the octahedral O first shell; SS from four Cr atoms, each sharing either two or three O atoms with the central Cr atom; SS from nine Cr atoms (sharing one O atom with the central Cr atom) at two different distances; MS within the first O shell. The sequential inclusion of these shells in the fit and the resulting parameters are shown in Figure 2 and Table 2. Constraints on the fit parameters resulted from initial systematic testing of unconstrained shells

TABLE 2: Results from Modeling Cr_2O_3, Cr-perchlorate (CrClO4-01-22), and Cr-acetate (CrAc100-01-28) Data[a]

sample	figure	shell	N	R (Å)	σ^2 (10^{-3} Å^2)	ΔE_0 (eV)	R-factor	χ_ν^2	ν
Cr_2O_3[b]	2b	O1	2 × 3[c]	1.98[c]	2.0 ± 1.4	6.9 ± 2.9	0.22	1126	19
Cr_2O_3[b]	2c	O1	2 × 3[c]	1.98[c]	1.9 ± 0.9	7.1 ± 1.4	0.09	511	17
		Cr1	1	2.65	2.7 ± 1.1	3.2 ± 3.1			
		Cr1	3	2.89	2.7 ± 1.1	3.2 ± 3.1			
Cr_2O_3[b]	2d	O1	2 × 3[c]	1.98[c]	2.0 ± 0.6	7.1 ± 0.8	0.03	177	16
		Cr1	1	2.65	3.1 ± 0.7	5.6 ± 1.1			
		Cr1	3	2.89	3.1 ± 0.7	5.6 ± 1.1			
		Cr2	3	3.43	3.9 ± 0.8	5.6 ± 1.1			
		Cr2	6	3.65	3.9 ± 0.8	5.6 ± 1.1			
Cr_2O_3[b,d]	2e	O1	2 × 3[c]	1.98[c]	2.0 ± 0.4	7.2 ± 0.5	0.016	94	16
		Cr1	1	2.65	3.1 ± 0.5	5.0 ± 0.8			
		Cr1	3	2.89	3.1 ± 0.5	5.0 ± 0.8			
		Cr2	3	3.43	3.6 ± 0.5	5.0 ± 0.8			
		Cr2	6	3.65	3.6 ± 0.5	5.0 ± 0.8			
CrClO4-01-22	3a	O1	6.1 ± 0.5	1.96 ± 0.01	0.6 ± 1.0	1.6 ± 1.1	0.041	256	17
CrClO4-01-22	3b	O1	5.8 ± 0.3	1.96 ± 0.01	0.2 ± 0.6	1.8 ± 0.6	0.020	91	14
		O2	13.7 ± 6.3	4.01 ± 0.03	20.9 ± 13.7	1.8 ± 0.6			
CrClO4-01-22	3a	O1	6.0 ± 0.4	1.96 ± 0.01	0.5 ± 0.7	1.2 ± 0.6	0.023	112	16
		MS[d]	0.64 ± 0.11						
CrClO4-01-22	3a	O1	7.0 ± 0.4	1.96 ± 0.01	1.5 ± 0.6	0.7 ± 0.6	0.011	57	14
		H	2 × N_{O1}	1.96 ± 0.01	3.4 ± 3.2	0.7 ± 0.6			
		MS[d]	0.67 ± 0.09						
CrAc100-01-28[e]	7a	O1	5.9 ± 0.6	1.98 ± 0.01	2.2 ± 1.0	5.5 ± 1.5	0.019	206	10
		Cr	2.8 ± 1.2	3.30 ± 0.03	5.2 ± 3.5	−1.6 ± 3.7			
CrAc100-01-28[f]	7b	O1	5.7 ± 0.4	1.96 ± 0.01	1.9 ± 1.0	1.4 ± 1.0	0.042	405	13
		Cr	18.9 ± 7.4	3.43 ± 0.04	30.7 ± 8.3	7.7 ± 1.7			
CrAc100-01-28[g]	7c	O1	5.8 ± 0.5	1.96 ± 0.01	2.2 ± 1.1	0.4 ± 0.9	0.031	363	12
		MS[d]	0.64 ± 0.18						
		Cr	3.2 ± 1.8	3.32 ± 0.05	7.3 ± 5.4	0.6 ± 4.8			
CrAc100-01-28[h]	7d	O1	5.8 ± 0.4	1.96 ± 0.01	2.2 ± 1.0	0.3 ± 0.8	0.030	350	14
		MS[d]	0.66 ± 0.17						
		Cr	2.6 ± 0.6	3.31 ± 0.02	5.2	0.3 ± 0.8			

[a] N, R, σ^2, and ΔE_0 are the parameters used to calculate the EXAFS contribution from the corresponding shell. Parameters for which deviations are not given are kept constant in the fits. Graphic fit results are shown in the corresponding figures. R-factor and χ_ν^2 are statistical parameters, and ν values are the degrees of freedom in the fit. [b] An expansion parameter α is used to vary the path length on the basis of the crystallographic distance: $R = R_o(1 + \alpha)$. Values for α were in the range (0.001−0.003). The amplitude factor S_0^2 was 0.69 ± 0.09 for the fit with O1 + Cr1 shells and was fixed to that value in all other fits. [c] Two separate shells at crystallographic distances of 1.96 and 2.01 Å were used in the fit. The quoted distance is the average. [d] Fit with first-shell MS included. All MS parameters were constrained to O1 shell SS parameters. If N is provided for an MS path, it represents an amplitude scaling factor. Explanations are given in the text. [e] Δk = 3.8−12.5 Å^{-1}. [f] Δk = 2.5−12.5 Å^{-1}. [g] Δk = 2.5−12.5 Å^{-1}, including MS from O1 shell. [h] Δk = 2.5−12.5 Å^{-1}, MS from O1 shell, constrained.

in isolated parts of the spectrum. A single lattice expansion variable was applied for all distances. The MS parameters were constrained to those of the first shell, under the assumption of uncorrelated atom movements.[33] The paths that were found necessary to fit the data represent the local crystallographic environment of the Cr atom, except for all O atoms that are outside the near-neighbor "O1" shell. The lack of signal from these O atoms is probably due to the expected large Debye−Waller (DW or σ^2) factor of these paths resulting from lattice vibrations in room-temperature measurements. Unlike the outer-shell O atoms, all detected Cr atoms share one to three first-shell "O1" atoms with the central Cr atom. The better-defined Cr−Cr distance, together with the generally larger backscattering amplitude of heavier atoms, results in detectable Cr contributions in the spectrum. The inclusion of MS from the first O shell significantly improved the fit quality at 2.8−4.0 Å. This observation demonstrates that first-shell MS can be significant in experimental data of octahedrally coordinated Cr.

Cr Perchlorate Solutions. The perchlorate anion is a weakly binding ligand, and no complexation with the Cr^{3+} ion is expected.[34] To test this expectation and to look for fluorescence self-absorption effects, the spectra at three $Cr(ClO_4)_3$ concentrations (0.05−0.2 M) were compared. No differences were observed, suggesting that the perchlorate anion is not bound to the metal in this concentration range. A 4% reduction in the nearest FT peak amplitude was observed in the 0.2 M sample relative to the 0.05 and 0.1 M samples. We conclude that even if self-absorption effects are present at 0.2 M Cr concentration, they are within the approximately 10% uncertainty in EXAFS first-shell amplitudes.

The FT of data from the 0.1 M Cr perchlorate solution are shown in Figure 3. The main peak at 1.5 Å was modeled by a single shell of O atoms. The resulting parameters are shown in Table 2. We observed an octahedral hydration sphere at 1.96 ± 0.01 Å, with very little disorder (σ^2 = 0.0006 Å^2). The sixfold coordination was not assumed in our model but was rather obtained as a result of the fit. The small disorder is indicative of the strong interaction between the Cr^{3+} ion and the water molecules, consistent with the long residence time obtained by NMR.[17] The distance and coordination numbers determined by XAFS are consistent with the octahedral shell at 1.97−1.98 Å determined by X-ray and neutron scattering and by other XAFS studies.[2,15,16] The distance is also in excellent agreement with electronic structure calculations (optimized Cr−H_2O distance of 1.965 Å).[35] Differences between experiment and model spectra observed at about 2.0 Å in the FT (Figure 3) can also be seen in modeling of the Cr_2O_3 standard (Figure 2). These differences could be attributed to systematic error in the Cr−O backscattering calculation, but they appear more pronounced in modeling of solution data. Addition of the H atoms from hydration water molecules significantly improved the fit (Figure 3d, Table 2), but the obtained distance of 2.30 Å was quite different from the 2.60 Å determined for the Cr−H correlation by neutron scattering.[4] The reason for the discrepancy could

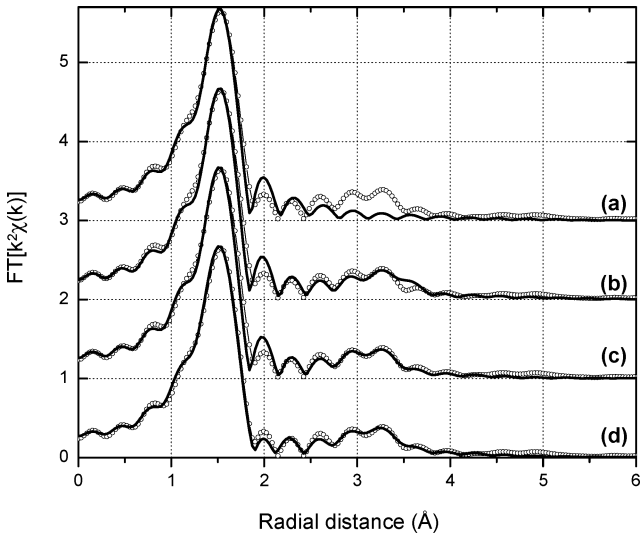

Figure 3. Fourier transforms of k^2-weighed data (circles) and fits (line) for the 0.1 M $Cr(ClO_4)_3$ solution. Transform and fit parameters are $\Delta k = 2.5-12.5$ Å^{-1} and $\Delta R = 1.0-4.0$ Å. Fits: (a) nearest-neighbor O1 shell only. (b) O1 and SS paths from O2 shell. (c) O1 and MS paths from O1 shell. (d) O1, H, and MS paths from O1 shell.

be inaccurate calibration of phase shifts for electron backscattering from the H atoms in the calculation. Modeling of the H shell also slightly affects O1 shell parameters (although within their uncertainties) and will need additional careful consideration. A future study will examine these differences, as a similar effect was observed in Cd perchlorate solutions.[36] Alternatively, electron backscattering from the O atoms could be slightly different in an aqueous environment than in a crystal oxide. (This alternative is supported by the fact that comparable differences between experiment and model at this distance are observed in modeling Cr acetate solutions, in which only one water molecule is present in the local environment. See Figure 7b−d.) Because the differences are localized in the Fourier transform and are of relatively small magnitude, they do not interfere with contributions at distances larger than about 2.2 Å. Thus, the conclusions presented below are not affected.

That a defined second hydration sphere is formed around Cr^{3+} was determined previously.[4,8,9,12,13,15,16] Perhaps the most convincing structural evidence is provided by neutron scattering, through analysis of both the Cr−O and Cr−H correlations in a double-difference isotopic substitution method.[4] In these studies, a second hydration shell is observed at a distance of about 4 Å, with a coordination number between 15 and 18. The ability of EXAFS to detect this shell in Cr solutions was examined in a series of studies,[14−16] by careful analysis of the structure observed at about 3.2 Å in the FT. The conclusion was that SS from a second hydration sphere is an important spectral contribution but that first-shell MS paths are also necessary to fit the data accurately. In later work, the role of second-shell SS in the high-R features was determined to be smaller than the effect of first-shell MS but still large enough to be detected and analyzed.[35,37,38] Other researchers have dismissed contributions of the second hydration shell in the EXAFS of aqueous ions on the basis of large disorder in the second hydration shell.[39,40] The apparent controversy and difficulty in interpretation arises because the distance to the second hydration molecules in Cr^{3+} is twice that to the first, so first-shell collinear MS contributions overlap second-shell SS ones in the FT.

Our data confirm the presence of FT structure at 3.2 Å in the spectra of all Cr perchlorate solutions (Figure 3). This structure becomes almost extinct when the lower FT limit is changed from 2.5 to 3.8 Å^{-1}, as seen previously.[15] We were able to model this part of the spectrum both by using SS from an outer O shell (Figure 3b, Table 2) and by using only MS within the tightly bound first hydration sphere (Figure 3c, Table 2). The MS model seems to fit the data better in the region at 3.0−3.7 Å. Additional support for an MS interpretation comes from our inability to observe SS from any O atoms other than the near-neighbor ones in the Cr_2O_3 powder standard. However, our fit results do not indicate that the MS model is statistically different from the second hydration SS model. Sakane et al.[16] compared the SS, MS, and a combination of the two models in fitting this part of a hydrated Cr^{3+} spectrum. An inherent limitation in MS modeling is the necessity to constrain the large number of variables. Employing the chosen constraints for the MS path parameters and the number of second-hydration-shell molecules, the authors concluded that a combined SS and MS model produced a superior fit than each model alone. We limited our analysis to testing either SS or MS contributions. In our MS model, the distance and the DW factors were constrained to the first-shell SS parameters in a way that ignores correlated atom motion.[33] The shape and phase of the features at 3.0−3.5 Å were reproduced correctly, but an amplitude variable for only MS contributions had to be introduced to fit the amplitude. The fit value of this variable (0.64 ± 0.11) shows that the actual amplitude of the MS features is about 35% smaller than predicted from the number of first coordination sphere molecules. Assuming for a moment that MS is the main contribution in this part of the spectrum, the origin of this amplitude reduction could be an overestimated electron mean free path in the XAFS calculation, correlated vibrations of first-shell water molecules (such as a "breathing" mode of opposite molecules, resulting in a different DW factor for MS paths), deviations from the 180° O1−Cr−O1 angle used in calculating the MS paths, or an unknown combination of these. An alternative explanation for the amplitude could be the presence of out-of-phase second-shell SS contributions, destructively interfering with the MS contribution and reducing the amplitude.

The limitations of MS modeling and the lack of information to account for the amplitude factors discussed above precluded a reliable SS versus MS analysis of this part of the spectrum. Recent studies employing ab initio electron structure calculations and molecular dynamics simulations have made significant progress in constraining the MS parameters in aqueous Cr^{3+} and determining the relative importance of SS and MS paths. On the basis of the adopted model, the contribution of second-shell SS is limited to about one-third of the total amplitude.[35,37,38] We present here an alternative approach for determining a contribution of SS paths from an outer hydration shell. Because the structure at 3.0−3.5 Å is, in general, a linear superposition of SS and MS paths, a reduction in the amplitude of each component should result in change of the overall amplitude. The amplitude parameters that are specific to a molecular configuration are the coordination number and the DW factor. One can thus anticipate a change in the overall amplitude when the number of second-hydration-shell molecules is reduced or when their disorder is increased. This can be the result, for instance, of an interfering anion in the second shell. The approach then is to fit accurately the observed structure at 3.0−3.5 Å in the experimental Cr perchlorate spectrum regardless of the SS or MS origin of the features, and look for amplitude differences in a case where the second hydration shell is disturbed.

Such a case is provided by the Cr acetate aqueous complex. As will be shown in the analysis for Cr acetate solutions, the

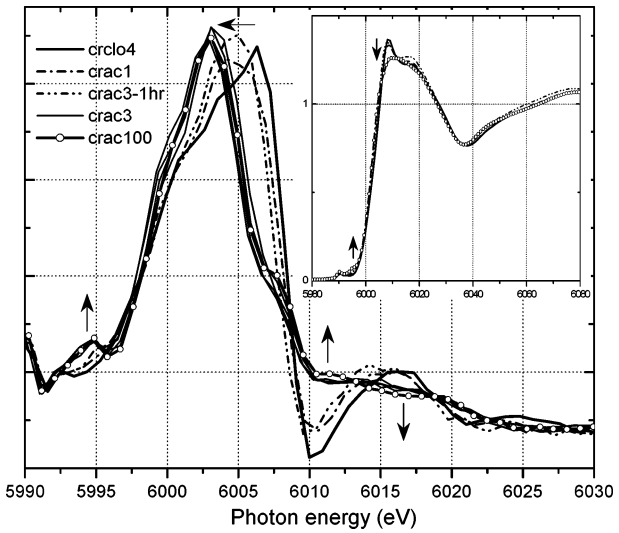

Figure 4. Derivative of normalized near-edge spectra (XANES) for 0.1 M Cr perchlorate (heavy line) and Cr acetate solutions. The broken lines show spectra for freshly prepared acetate:Cr = 3 and aged acetate:Cr = 1 solutions. The multiple thin lines show similar spectra for all aged acetate:Cr = 3 solutions. Symbols show the spectrum for sample CrAc100−01−28. Arrows indicate the effect of increased acetate binding relative to the hydrated Cr spectrum. Inset: normalized XANES.

SS or MS features at 3.0−3.5 Å in the Cr perchlorate spectrum are present with the *same amplitude* in spectra for solutions having the trichromium acetate structure (Figure 1e). The number of second hydration molecules around each Cr atom should be reduced in the acetate solutions because of spatial considerations. In addition, the acetate groups in the structure of Figure 1e are likely to significantly broaden the distribution of $Cr-H_2O_{II}$ distances. Charge compensation by the acetate groups will also reduce the polarizing ability of the Cr^{3+} ion, diminishing the strength of the interactions and further broadening the distribution. The result of any of the above would be reduced or null amplitude of contributions assigned to second-shell hydration molecules. It is difficult to estimate the amount of the reduction, but the presented arguments indicate that it is likely to be significant. Assuming complete absence of second-shell SS in the Cr acetate spectra and using the 35% estimate for the SS relative contribution,[35,37,38] we obtain a maximum possible amplitude change of 35%. We did not observe any amplitude change in the Cr acetate samples, suggesting that the 3.0−3.5 Å structure in the Cr perchlorate spectra is due to MS. This conclusion is supported by the fact that the Cr first-shell environment in the Cr acetate complex is similar to that of hydrated Cr^{3+} ions, leading to the same MS contributions in the spectra.

Chromium Acetate Solutions. Figure 4 shows the derivative of near-edge (XANES) spectra for the Cr perchlorate solution and several acetate solutions. Significant differences relative to the hydrated Cr spectrum are observed with increasing fraction of acetate-bound Cr^{3+} ions in solution. When the acetate solutions are not aged or the acetate:Cr ratio is less than 3, the spectra are intermediate between hydrated and acetate-bound. Spectra cross at isosbestic points, indicating transition of equilibrium between only two distinct species.

The XANES part of the spectrum is sensitive to changes in the local potential at the Cr atom site.[27] The magnitude of change between the XANES of hydrated and acetate-bound Cr is larger than that seen for metals that form mononuclear acetate complexes, such as Cu^{2+}, Cd^{2+}, and Pb^{2+}.[23] This observation suggests that the local potential is modified because of atoms more polarizing than O or C in the local Cr environment, and is thus consistent with a polynuclear Cr structure.

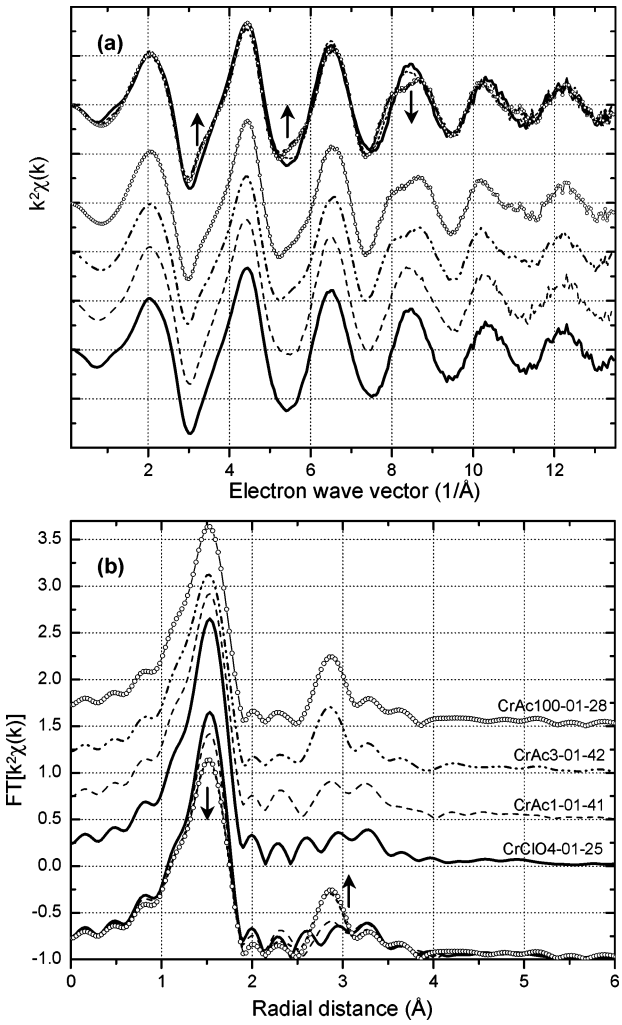

Figure 5. (a) k^2-weighed $\chi(k)$ from 0.1 M Cr perchlorate and aged Cr acetate solutions of different acetate:Cr ratios. (b) FT of data in (a), $\Delta k = 2.5-12.5$ Å^{-1}. Spectra are shifted vertically for clarity and are shown together at bottom of graph. The same line convention is used in a and b. Crac10 data (not shown) are the same as crac3/crac100 data. Arrows point at trends concurrent with Cr−acetate binding.

Qualitative EXAFS Analysis. As mentioned in the Introduction, a series of 0.1 M Cr acetate solutions has been studied extensively by using FT-IR, NMR, and mass spectrometry.[21] The spectra show dependence on the pH and acetate:Cr ratio of the solution. Evolution in the spectra can be seen during the first 70 h. The speciation diagram derived for aged solutions from the results of all methods shows that when the pH is in the range 4.0−5.5 and the acetate:Cr ratio is 3 or higher, the cyclic Cr acetate trimer (Figure 1e) is the predominant species in solution. Above pH 5.5, substitution of OH groups for bridging acetate groups is proposed, leading to the formation of a linear chromium triacetate chain (Figure 1B of Tackett[21]). For aged solutions with acetate:Cr ratio = 1, mononuclear bidentate complexes are suggested as the predominant species.

Effect of Age and Acetate:Cr Ratio. Figure 5 shows the XAFS spectra and FTs from aged 0.1 M Cr solutions. Though only two are shown, spectra of all aged samples having acetate:Cr ratio of 3 or higher are similar and display a prominent peak at 2.8 Å, in addition to the high-*R* features observed in the hydrated Cr spectrum. We attribute the additional peak to Cr−Cr coordination in a trichromium acetate structure, consistent with previous results.[21] Numerical modeling of the EXAFS confirms

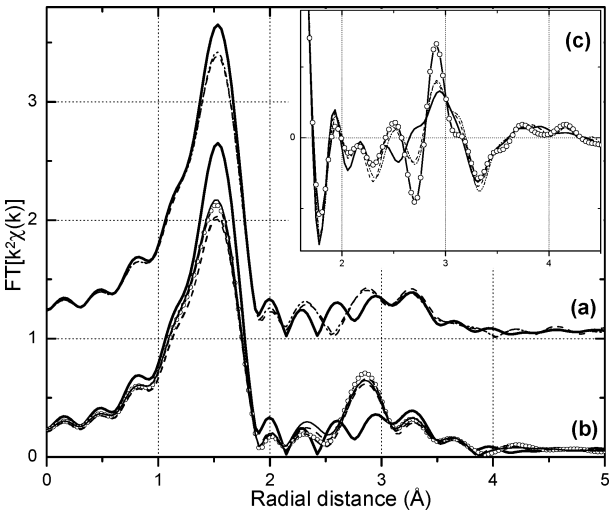

Figure 6. Fourier transforms of $k^2\chi(k)$ data showing the effects of aging, acetate:Cr ratio, and concentration. The hydrated Cr data (heavy line) are shown in all panels for reference. Transform range is Δk = 2.5−12.5 Å^{-1}. (a) Fresh acetate:Cr = 3 (dash) and aged acetate:Cr = 1 (dash−dot) solutions, 0.1 M. (b) Aged acetate:Cr = 3 solutions. Cr concentrations are 0.3 M (broken lines, pH 6.2 and 4.8) and 0.1 M (circles for pH 6.8, thin solid line for pH 4.2). (c) Imaginary part of data in a, together with the aged acetate:Cr = 3 solution of pH 4.2 (circles) from b.

our qualitative assignment (see below). Concurrently with the increase in amplitude of the peak at 2.8 Å, we observe a small decrease in the nearest-neighbor O peak at 1.5 Å. The imaginary part of the FT in the region 1.6−4.5 Å is shown in Figure 6. Significant differences in the phase and amplitude of the features are observed only in the region 2.4−3.2 Å, where the Cr−Cr interaction contributes.

Spectra taken from a freshly prepared (1-h) acetate:Cr = 3 sample and an aged acetate:Cr = 1 sample are identical (Figure 6a, c). The small changes observed relative to the hydrated Cr spectra resemble the initial formation of the peak at 2.8 Å in the aged acetate:Cr = 3 sample and can be interpreted as a small fraction of the Cr atoms forming the trichromium complex, while the rest remain hydrated ions. For the fresh acetate:Cr = 3 sample (CrAc3-01-420), this interpretation is consistent with the slow kinetics (on the order of days) of Cr acetate trimer formation.[21] For the spectrum of the aged acetate:Cr = 1 sample, such interpretation suggests the absence of the mononuclear bidentate binding proposed by Tackett[21] as predominant under these conditions. This last conclusion is supported by lack of spectral features from the C atom and from MS in the metal−C−CH_3 axis of a bidentate CH_3COO−Me complex (see Figure 1c). Spectra of the bidentate acetate complexes of Cd^{2+}(aq) and Pb^{2+}(aq) show prominent SS and MS features from C and CH_3 atoms, owing to the well-defined metal−C distance and the metal−C−CH_3 alignment.[36,41] We also did not observe spectral features from C atoms in the bridging acetate configuration of Cr (Figure 1e). This finding can be rationalized by the rotational degree of freedom of the acetate groups around an axis through the two O atoms in the COO. Large metal−C distance distributions resulting from rotation will destroy the coherence of backscattering coming from C and CH_3 atoms.

Effect of pH. Figure 6b shows spectra from samples at pH 4.2 and 6.8, for two Cr concentrations, 0.1 and 0.3 M. All spectra are identical, except for a small amplitude reduction at higher concentrations attributed to fluorescence self-absorption. This result suggests that the cyclic structure is preserved at pH 6.8. In the proposed linear complex at high pH,[21] the average Cr−Cr coordination is reduced by 33% relative to the cyclic structure. The linear structure can also be assumed to be more flexible, resulting in a Cr−Cr distance that is less well defined. Both factors will cause significant amplitude reduction in the FT peak centered at 2.8 Å. From the lack of such reduction, we conclude that the cyclic structure is retained, although it is possible that OH^- groups substitute for acetate groups at high pH. Differences between the spectra from all aged Cr acetate solutions with acetate:Cr ratios of 3 or more are negligible in the pH range 2.8−6.8. This is an indication that no substantial change in structure occurs because of possible hydrolysis. Although hydrolysis constants[42] suggest the formation of a $Cr_3(OH)_4^{5+}$ polymer in the absence of acetate, the FT-IR spectroscopy data clearly indicate that the acetate groups are bound to the Cr^{3+} ion.[21] The FAB mass spectrometry and ion exchange results in the same study are also consistent with the mass and +1 charge of a Cr_3OAc_6 complex.

Effect of Concentration. As mentioned earlier, we found no difference in local structure for aged acetate:Cr = 3 solutions of 0.1 and 0.3 M Cr concentrations. A dilute 0.03 M sample (CrAc10-003-35) yielded data of lower quality but showed no significant difference from the 0.1 M sample (CrAc10-01-35).

Qualitative Conclusions. The qualitative EXAFS analysis showed that over a wide range of experimental conditions the only structure observed by XAFS was a Cr acetate polymer. The conditions included samples ranging in Cr concentration from 0.03 to 0.3 M and pH changes from 2.8 to 6.8 (above and below which a structural transition has been suggested[21]). When the solution had not aged or only one acetate group was available per Cr^{3+} ion, the local Cr environment consisted predominantly of hydration molecules. Spectra cross at isosbestic points (Figure 6c), indicating a linear combination of only two local environments around Cr: hydrated and acetate-bound species. We thus modeled only the end members of the series: a Cr perchlorate ($CrClO_4$-01-25, see above) sample and a Cr acetate (CrAc100-01-28) sample, representative of the hydrated and acetate-bound species, respectively.

EXAFS Modeling. Data from sample CrAc100-01-28 were fitted in *R*-space simultaneously at three FT *k*-weightings (FT-[$k^n\chi(k)$], n = 1, 2, 3).[43] This approach to the fitting takes advantage of the differences in the backscattering amplitude of heavier (e.g., Cr) and lighter (e.g., O, C) atoms, without overemphasizing any one of them as could happen in single *k*-weighting fits. It can also enable further decoupling of the correlations between the XAFS coordination number and DW factor parameters for individual backscattering shells.

As an initial step, the data were fitted with the lower FT range limit set to 3.8 Å^{-1}. This was done to filter out the low-*k* contribution mentioned in the analysis of the hydrated Cr samples, which appears as structure around 3.2 Å in the FT. The O and Cr shells appear well resolved in the FT, and modeling them as such produced an excellent fit (Figure 7a and Table 2). The Cr−O distance is close to that obtained for the hydrated Cr sample. The Cr−O DW factor is very small, indicating strong binding. Its slightly larger value than that of the hydrated sample most likely results from the three different types of O atoms present in the octahedral coordination around Cr (i.e., four O atoms from the bridging acetate groups, one central O atom, and one water molecule). Though it is surprising that different types of O atoms in a shell would not cause more disorder, the Cr^{3+} ions seem to have very strong, similar interactions with water molecules, with atomic O, or with O atoms in the carboxyl group. The Cr−Cr distance obtained from fits of the XAFS data is consistent with the 3.28 Å determined

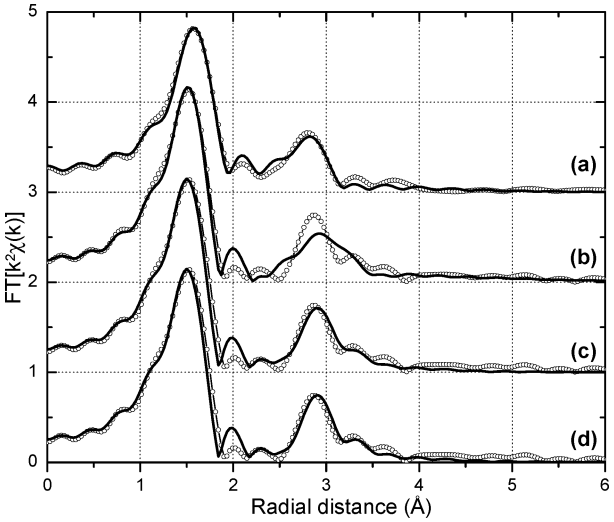

Figure 7. Fourier transforms of $k^2\chi(k)$ data (circles) and fits (line) for the CrAc100−01−28 solution. Transform and fit parameters are $\Delta k = 2.5-12.5$ Å^{-1} (except for a, where $\Delta k = 3.8-12.5$ Å^{-1}) and $\Delta R = 1.0-4.0$ Å. Fits: (a) O and Cr shells. (b) O and Cr shells. (c) O and Cr shells, with MS paths from O shell, unconstrained. (d) O and Cr shells, with MS paths from O shell, constrained as explained in text.

in crystalline $6H_2O{\cdot}[OCr_3(CH_3COO)_6{\cdot}3H_2O]^+Cl^-$.[22,44] The Cr−Cr coordination number (2.8 ± 1.2) is larger than but consistent with the 2.0 expected for the trichromium acetate structure. The reason for the larger coordination number could be correlation of this variable with the DW factor because of the limited data range, resulting also in the large error bars on the parameters. The Cr atoms in the acetate structure are at similar distances and in similar binding geometries (sharing one O atom) as the Cr2 atoms in Cr_2O_3 (Table 2). If the Cr−Cr DW factor in the fits of the Cr acetate data is set to the value obtained for Cr2 atoms in the Cr_2O_3 fits, we obtain a coordination number of 2.2, closer to the theoretical 2.0 for a trichromium acetate complex. Overall, with these two shells the data are fitted well at all three *k*-weightings, and the major contributions in the XAFS spectrum of this sample are determined.

When the lower FT limit is set to 2.5 Å^{-1}, the quality of the fit around 2.8 Å in *R*-space is degraded, and fit parameters become unrealistic (Figure 7b, Table 2). A Cr shell alone is insufficient to fit the data. A closer analysis of the imaginary part of the FT (Figure 6c) reveals that the acetate spectrum is almost identical to the perchlorate spectrum outside the range 2.5−3.1 Å. The features in that region show that with increasing acetate binding, an increasing contribution is added to a constant "baseline". As argued in the Cr perchlorate analysis, either a second-hydration-shell SS path or first-shell MS paths can be used to fit the "baseline" part of the data equally well. We chose to include first-shell MS paths in the analysis of the acetate solution, in addition to the Cr contribution. The MS paths were constrained to the first O shell SS parameters, and a scaling variable was used as in the Cr perchlorate analysis. Results of this model are shown in Figure 7c and Table 2. The Cr and MS contributions overlap in *R*-space, resulting in large correlations between dependent variables (typically $R - \Delta E_0$ and $N - \sigma^2$). On the basis of the results of this "unconstrained" fit, all ΔE_0 variables were constrained to be equal, and the DW factor for the Cr shell was set to the one obtained when the MS contributions were filtered out (i.e., 0.0052 Å^2). Results of this final model are given in Figure 7d and Table 2.

The refined parameters obtained from the constrained model allow us to make two observations. First, we recovered structural information for the Cr shell obtained when the "second hydration/multiple scattering" shell signal was filtered out. Despite the overlap in *R*-space of the MS and Cr shell contributions, the fact that the imaginary part of one is rapidly oscillating, whereas the other varies slowly and over a wider *R*-range, allows differentiation between the two and makes extraction of the quantitative information possible. Each Cr atom has 2.6 ± 0.6 Cr neighbors, supporting the cyclic Cr polymer structure in solution. (When the DW factor was set to the value obtained for Cr2 atoms in the Cr_2O_3 fits, as justified earlier, we obtained a coordination number of 2.2.) The latter is further supported by the relatively small DW factor for a second-shell Cr−Cr interaction; a linear arrangement would allow more flexibility than a cyclic one. Second, the scaling factor obtained for first-shell MS contributions is the same as that obtained in fitting of the high-*R* region of the hydrated Cr sample with the same paths. This means that the "second hydration shell/multiple scattering" contribution has the same amplitude in both the hydrated Cr sample and the Cr acetate trimer. Considering the quite different structures in the two cases, a reduction or complete absence of the contribution by the second hydration shell is expected in the Cr acetate solutions versus the hydrated Cr solutions. This expectation follows from the fact that the space around each Cr atom lying on the inside of the trimer structure is inaccessible to outside water molecules (Figure 1e). The $Cr_3O(Ac)_6$ structure is also likely to increase the disorder in an outer hydration shell around each Cr, further reducing the amplitude. We observe no change of this signal in the Cr acetate spectra relative to the hydrated Cr spectra. Therefore, these features must be due to MS within the first coordination sphere of the Cr atom. This conclusion is strengthened by the similar parameters for the first O shell obtained in fitting of both the hydrated Cr and the Cr acetate solution data. The octahedral first-shell environment in both samples is likely to produce similar MS effects. The possibility of contributions from the acetate groups compensating the lack of second-hydration-shell contributions in Cr acetate spectra can be dismissed on the basis of the lack of features from C atoms discussed earlier in the qualitative analysis.

Summary

The distinct Cr−Cr interaction in the XAFS spectra indicates that a Cr polymer structure is the dominant species in aqueous acetate solutions with acetate:Cr ratios of 3 or higher. The spectra are unchanged when pH is varied in the range 2.8−6.8 or the Cr concentration is changed from 0.03 to 0.3 M. Only a small fraction of the Cr^{3+} ions are complexed when solutions are not aged sufficiently or when only one acetate group per Cr^{3+} ion is available. In the latter case, we did not observe the mononuclear bidentate binding suggested in previous studies. Modeling of the data corroborates previous findings that Cr forms a $Cr_3O(Ac)_6$ cyclic polymer in acetate solutions. The similarity of spectra regardless of pH indicates preservation of the cyclic complex and lack of structural transition to a linear Cr polymer with increased pH. However, substitution of OH^- for acetate groups in the cyclic structure with increased pH could not be ruled out. Incorporation of MS contributions because of the first Cr−O shell enabled an accurate fit of hydrated Cr data at a distance of 3.0−3.5 Å in the FT. In modeling data from Cr acetate solutions, the same contributions needed to be included with the same amplitude. This allowed us to clarify the origins of the features at 3.0−3.5 Å and attribute them entirely to MS in the first shell. Therefore, backscattering from the outer water molecules in the Cr^{3+} hydration structure could not be identified in the EXAFS spectrum.

This and other studies show that XAFS is a sensitive technique for investigating metal hydration and complexation structures at environmentally relevant concentrations. Such information can help in studies of the binding of dilute aqueous Cr to carboxyl ligands (e.g., in cell walls, Langmuir monolayers, micelles, and cell exudates), as well as in investigations of metal−metal interactions and polymerization in solution. Formation of the Cr acetate polymer can be a factor in Cr transport when dissolved acetate groups are present, as it can significantly affect reactivity and partitioning.

Acknowledgment. M.B. acknowledges support from the Environmental Molecular Science Institute at University of Notre Dame (funded by NSF grant EAR-0221966), the United States Department of Energy, and the Bayer Corporation through a fellowship in environmental science. Help in beamline setup from the staff of MRCAT is greatly appreciated, as is use of the laboratory of J. Fein. We would like to thank M. Duncan for the editorial handling and the reviewers for their comments. This work was supported in part by National Science Foundation grant EAR-0207169 and EAR-9905704, and the U.S. Department of Energy, Office of Science, Office of Biological and Environmental Research, Natural and Accelerated Bioremediation program. MRCAT is supported by the U.S. Department of Energy under Contract DE-FG02-94-ER45525 and the member institutions. Use of the Advanced Photon Source was supported by the U.S. Department of Energy, Office of Science, Office of Basic Energy Sciences, under Contract W-31-109-Eng-38.

References and Notes

(1) Ohtaki, H. Structure and dynamics of solutions. In *Structure and dynamics of solutions*; Ohtaki, H., Yamatera, H., Eds.; Elsevier: Amsterdam, 1992; Chapter 2.
(2) Ohtaki, H.; Radnai, T. *Chem. Rev.* **1993**, *93*, 1157.
(3) Marcus, Y. *Chem. Rev.* **1988**, *88*, 1475.
(4) Broadbent, R. D.; Neilson, G. W.; Sandstrom, M. *J. Phys.: Condens. Matter* **1992**, *4*, 639.
(5) Lindqvist-Reis, P.; Munoz-Paez, A.; Diaz-Moreno, S.; Pattanaik, S.; Persson, I.; Sandstrom, M. *Inorg. Chem.* **1998**, *37*, 6675.
(6) Magini, M. *J. Chem. Phys.* **1980**, *73*, 2499.
(7) Caminiti, R.; Licheri, G.; Piccaluga, G.; Pinna, G. *Chem. Phys.* **1977**, *19*, 371.
(8) Read, M. C.; Sandstrom, M. *Acta Chem. Scand.* **1992**, *46*, 1177.
(9) Caminiti, R.; Licheri, G.; Piccaluga, G.; Pinna, G. *J. Chem. Phys.* **1978**, *69*, 1.
(10) Bol, W.; Welzen, T. *Chem. Phys. Lett.* **1977**, *49*, 189.
(11) Bergstrom, P. A.; Lindgren, J.; Read, M.; Sandstrom, M. *J. Phys. Chem.* **1991**, *95*, 7650.
(12) Bleuzen, A.; Foglia, F.; Furet, E.; Helm, L.; Merbach, A. E.; Weber, J. *J. Am. Chem. Soc.* **1996**, *118*, 12777.
(13) Easteal, A. J.; Mills, R.; Woolf, L. A. *J. Phys. Chem.* **1989**, *93*, 4968.
(14) Diaz-Moreno, S.; Munoz-Paez, A.; Martinez, J. M.; Pappalardo, R. R.; Marcos, E. S. *J. Am. Chem. Soc.* **1996**, *118*, 12654.
(15) Munoz-Paez, A.; Pappalardo, R. R.; Marcos, E. S. *J. Am. Chem. Soc.* **1995**, *117*, 11710.
(16) Sakane, H.; Munoz-Paez, A.; Diaz-Moreno, S.; Martinez, J. M.; Pappalardo, R. R.; Marcos, E. S. *J. Am. Chem. Soc.* **1998**, *120*, 10397.
(17) Cusanelli, A.; Frey, U.; Richens, D. T.; Merbach, A. E. *J. Am. Chem. Soc.* **1996**, *118*, 5265.
(18) Tackett, J. E. *Appl. Spectrosc.* **1989**, *43*, 483.
(19) Deacon, G. B.; Phillips, R. J. *Coord. Chem. Rev.* **1980**, *33*, 227.
(20) Nakamoto, K. *Infrared and Raman spectra of inorganic and organic coordination compounds*, 4th ed.; Wiley: New York, 1986.
(21) Tackett, J. E. *Appl. Spectrosc.* **1989**, *43*, 490.
(22) Chang, S. C.; Jeffreey, G. A. *Acta Crystallogr., Sect. B* **1970**, *B26*, 673.
(23) Boyanov, M. I.; Shibata, T.; Kelly, S. D.; Kemner, K. M.; Bunker, B. A. Spectral features in the XAFS of aqueous metal-acetate complexes. Presented at the XAFS 12 conference in Malmo, Sweden, May 2003; Abstract A7400, p 169.
(24) Segre, C. U.; Leyarovska, N. E.; Chapman, L. D.; Lavender, W. M.; Plag, P. W.; King, A. S.; Kropf, A. J.; Bunker, B. A.; Kemner, K. M.; Dutta, P.; Duran, R. S.; Kaduk, J. The MRCAT insertion device beamline at the Advanced Photon Source. In *Synchrotron Radiation Instrumentation: Eleventh U.S. National Conference*; Pianetta, P., Ed.; American Institute of Physics: New York, 2000; Vol. CP521, p 419.
(25) Kemner, K. M.; Kropf, J.; Bunker, B. A. *Rev. Sci. Instrum.* **1994**, *65*, 3667.
(26) Cross, J. O.; Frenkel, A. I. *Rev. Sci. Instrum.* **1999**, *70*, 38.
(27) Koningsberger, D. C.; Prins, R. *X-ray Absorption: Principles, Applications, Techniques of EXAFS, SEXAFS, and XANES*; Wiley: New York, 1988.
(28) Newville, M.; Livins, P.; Yacoby, Y.; Rehr, J. J.; Stern, E. A. *Phys. Rev. B* **1993**, *47*, 14126.
(29) Ankudinov, A. L.; Ravel, B.; Rehr, J. J.; Conradson, S. D. *Phys. Rev. B* **1998**, *58*, 7565.
(30) Ravel, B. *J. Synchrot. Radiat.* **2001**, *8*, 314.
(31) Newville, M.; Ravel, B.; Haskel, D.; Rehr, J. J.; Stern, E. A.; Yacoby, Y. *Physica B* **1995**, *208−209*, 154.
(32) Wyckoff, R. W. G. *Crystal Structures*; John Wiley & Sons: New York, 1964; Vol. 2.
(33) Haskel, D. Local Structural Studies of Oriented High-Temperature Superconducting Cuprates by Polarized XAFS Spectroscopy. Ph.D. Dissertation, University of Washington, 1998; p 256.
(34) Martell, A. E.; Smith, R. M. *Critical Stability Constants*; Plenum Press: New York, 1974; Vol. 1−5.
(35) Campbell, L.; Rehr, J. J.; Schenter, G. K.; McCarthy, M. I.; Dixon, D. *J. Synchrot. Radiat.* **1999**, *6*, 310.
(36) Boyanov, M. I.; Kelly, S. D.; Kemner, K. M.; Bunker, B. A.; Fein, J. B.; Fowle, D. A. *Geochim. Cosmochim. Acta* **2003**, *67*, 3299.
(37) Merkling, P. J.; Munoz-Paez, A.; Marcos, E. S. *J. Am. Chem. Soc.* **2002**, *124*, 10911.
(38) Merkling, P. J.; Munoz-Paez, A.; Martinez, J. M.; Pappalardo, R. R.; Marcos, E. S. *Phys. Rev. B* **2001**, *6401*.
(39) Filipponi, A.; Dangelo, P.; Pavel, N. V.; Dicicco, A. *Chem. Phys. Lett.* **1994**, *225*, 150.
(40) Benfatto, M.; Natoli, C. R.; Bianconi, A.; Garcia, J.; Marcelli, A.; Fanfoni, M.; Davoli, I. *Phys. Rev. B* **1986**, *34*, 5774.
(41) Boyanov, M. I.; Kmetko, J.; Shibata, T.; Datta, A.; Dutta, P.; Bunker, B. A. *J. Phys. Chem. B* **2003**, *107*, 9780.
(42) Baes, C. F.; Mesmer, R. E. *Hydrolysis of Cations*; Wiley: New York, 1973.
(43) Kelly, S. D.; Kemner, K. M.; Fein, J. B.; Fowle, D. A.; Boyanov, M. I.; Bunker, B. A.; Yee, N. *Geochim. Cosmochim. Acta* **2002**, *66*, 3855.
(44) Figgis, B. N.; Robertson, G. B. *Nature (London)* **1965**, *205*, 694.